CHINESE OPTICS LETTERS

Vol. 21, No. 3 | March 2023

# Polarization domains and self-mode-locked pulses in an erbium-doped fiber laser

Peiyun Cheng (程佩芸)[1], Mengmeng Han (韩孟孟)[1], Yueqing Du (杜岳卿)[2], and Xuewen Shu (舒学文)[1*]

[1] Wuhan National Laboratory for Optoelectronics & School of Optical and Electronic Information, Huazhong University of Science and Technology, Wuhan 430074, China

[2] Key Laboratory of Light Field Manipulation and Information Acquisition, Ministry of Industry and Information Technology, Shaanxi Key Laboratory of Optical Information Technology, School of Physical Science and Technology, Northwestern Polytechnical University, Xi'an 710129, China

*Corresponding author: xshu@hust.edu.cn

Received August 3, 2022 | Accepted September 20, 2022 | Posted Online November 8, 2022

**We have observed various polarization domains and a giant self-mode-locked pulse in a 130 m long erbium-doped fiber laser without any mode-locking devices. By adjusting the intracavity polarization controller, we investigated the evolution process of the polarization domain with the varying cavity birefringence. When the birefringence was close to zero, the polarization domains split into multidomains, and finally a giant self-mode-locked pulse formed for the first time. We analyzed that the generation of the self-mode-locked pulse was related to the multiple subdomains ascribed to the strong coherent cross coupling between the orthogonal polarization light components in the long fiber cavity.**

**Keywords:** fiber lasers; polarization domains; self-mode-locked pulse; nonlinear optics.

**DOI:** 10.3788/COL202321.031402

## 1. Introduction

Ultrafast fiber lasers have gathered much attention because of their wide application prospects in the fields of laser machining, fiber communication, biochemistry, and metrology. In addition, fiber lasers can also serve as a perfect experimental platform for studying complex nonlinear dynamics processes. In general, the generation of pulses is mainly achieved by mode-locking techniques[1–5] in fiber lasers, and it is generally necessary to insert an optical modulator, a saturable absorber, an intensity- or polarization-dependent device in the cavity to achieve mode locking. However, even without any modulation devices or polarization-dependent devices, some fiber lasers can still pulsate at the fundamental frequency of the cavity[6–32]. Among them, polarization domains (PDs) and polarization domain walls (PDWs) have captured great interest. The typical feature of such pulses is that the polarization of light is periodically switched between two orthogonal directions at round-trip frequency. And for practical applications, PDs were studied to achieve the square-shaped pulse[15–19] and have been used in optical fibers as topological bits for data transmission[23]. Due to the existence of birefringence in fiber, the fundamental mode contains two orthogonal polarization modes with different propagation constants. PDW pulses are obtained due to the cross coupling of the two orthogonal polarization modes[6–22]. In 2009, Zhang *et al.*[6] first experimentally observed PDW solitons in weakly birefringent cavity fiber lasers, which were formed due to the strong coherent cross-polarization coupling of light in the fiber lasers. Subsequently, they achieved incoherent vector dark domain wall solitons in fiber lasers[7,8]. When considering the fiber birefringence-induced spectral filtering effect and the gain competition caused antiphase dynamics in fiber cavities, the coupled Ginzburg–Landau equation can well explain the formation of PDWs[8]. In 2014, Tang *et al.*[9] demonstrated that the PDW is a general feature in quasi-isotropic fiber laser cavities, which can be achieved under the incoherent and coherent coupling between two polarization supermodes. Highly nonlinear fibers and different kinds of saturable absorbers were used in fiber lasers to enhance the nonlinear effect, which were favorable for the cross coupling between the two polarization beams to achieve the PDWs[12–16]. Meanwhile, various PD and PDW states in different fiber lasers have been widely reported. The pulse durations of the PDs can be changed with the variation of the cavity parameters, and the PDWs are usually formed as bright pulses, dark pulses, or bright-dark pulse pairs with different temporal profiles[12–19]. Under a certain cavity condition, the PDs will split to form irregularly distributed multidomains[15–17], harmonic PDWs[18], or evolve into other types of pulses[20,22]. The research shows that the strength of the coherent or incoherent cross coupling can induce various domain states. The coherent coupling is more easily achieved in weak birefringence fiber cavities, while the incoherent coupling is generally obtained when the birefringence is strong[9]. Overall, the birefringence, as a key factor affecting coupling

strength, plays an important role in the generation and the properties of PDs and PDWs in fiber lasers. However, the detailed evolution process of the PD pulses varying with the changes of the intracavity birefringence in fiber lasers has rarely been reported.

In addition to PDs and PDWs, other types of self-mode-locked pulses are often observed in fiber lasers due to various optical mechanisms[24–32]. For example, the self-phase modulation and the longitudinal modes beating in the fiber cavity can lead to the occurrence of mode locking in the laser[24,25]. The gain fiber, such as erbium-doped fiber[26–29] and thulium-doped fiber[30–33], can also be used as both gain medium and saturable absorber to realize self-$Q$-switching or self-mode locking, which results from the energy transfer processes such as ion pairs excited state absorption[32] and upconversion interaction[33]. These studies show that the operation mechanisms of self-pulses in fiber lasers are complex, which is worth further exploration. It is also important to study the internal relationship between different types of self-pulses and whether they can be realized in the same laser, which can deepen our understanding of the pulsation mechanisms of fiber lasers. However, there have been few reports on it.

In this paper, we report various PDs and a self-mode-locked pulse observed in a 130 m erbium-doped fiber laser without any mode lockers. Incoherently coupled PDs with different temporal and spectral distributions and harmonic PDs have been obtained in this fiber laser by adjusting the pump power and the polarization controller (PC). By fine-tuning the intracavity PC, we studied the detail evolution of the PDs with the cavity birefringence decreasing. When the birefringence was gradually close to zero, the PDs split and eventually evolved into a giant self-mode-locked pulse. The self-mode-locked pulse possessed high pulse energy and was quite stable. Based on the experimental results, we analyze that the giant self-mode-locked pulse originated from the multiple subdomain pulses, which resulted from the strong coherent coupling between two polarization modes in the long fiber cavity. We experimentally studied the PDs evolution process with the intracavity birefringence varying, realized the PDs and the self-mode-locked pulse in the same fiber cavity, and found the correlation between them for the first time.

## 2. Experimental Setup

The configuration of the fiber laser used in our experiment is shown in Fig. 1. The laser pump source was a 980 nm laser diode (LD) with a maximum pump power of 500 mW. A 980/1550 wavelength-division multiplexer (WDM) was applied to couple the pump light into the laser cavity. The gain medium, a 5 m erbium-doped fiber (EDF, Fibercore I-25), was inserted into the cavity. The group velocity dispersion of the EDF was $-29\ \mathrm{ps}^2/\mathrm{km}$. The light was extracted from the cavity for monitoring through a 50:50 output coupler (OC1). A polarization-insensitive optical isolator (ISO) forced the light to propagate unidirectionally. An intracavity PC1 was used to adjust the

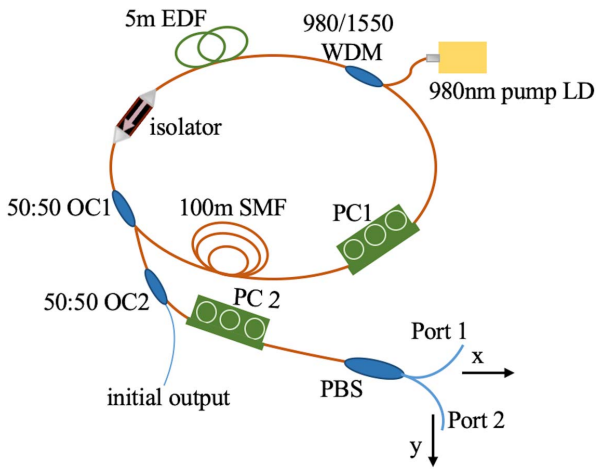


**Fig. 1.** Schematic of the experimental fiber laser structure.

birefringence in the fiber cavity. In addition to the EDF and ~5 m SMF pigtail fiber introduced by other optical components in the cavity, there was a piece of 120 m standard single-mode fiber (SMF) with a group velocity dispersion of $-22\ \mathrm{ps}^2/\mathrm{km}$ in the cavity. The total length of the cavity was ~130 m. The net dispersion was about $-2.895\ \mathrm{ps}^2$. The output laser was split by a 50:50 OC2. One port of the OC2 was used to observe the initial pulse output from the fiber laser, and another port was used to monitor the two orthogonal polarization components, which were separated by a fiber-optic polarization beam splitter (PBS) for studying the vector nature of the pulse. The PC2 was used to offset the linear polarization caused by the pigtail fiber outside the cavity. A 500 MHz oscilloscope, together with a 5 GHz photodetector and an optical spectrum analyzer, was used to detect and monitor the light extracted from the laser cavity.

## 3. Experimental Results

When the pump power reached the laser threshold of 65 mW, the fiber cavity realized continuous-wave laser output. By increasing the pump power and adjusting the PC1, the PDs were observed with the threshold pump power of 125 mW, as presented in Fig. 2(a). The repetition frequency was 1.58 MHz, corresponding to the cavity length of 130 m. Figure 2(a) shows the PD pulse trains of the horizontal axis and the vertical axis components; the widths of the domains along the two orthogonal directions are about 75 ns and 520 ns, respectively. The polarization of the output light was periodically switched between the two orthogonal directions. The PDW appeared as a bright pulse at a polarization switching position and separated the two PDs. The spectra of the PD pulses are shown in Fig. 2(b). The two orthogonal components had the central wavelengths at 1573.13 and 1572.84 nm, respectively. The spectral profiles of the two polarization components were different, indicating that the coupling between the two polarization modes was incoherent. The wavelength difference was about 0.29 nm, which

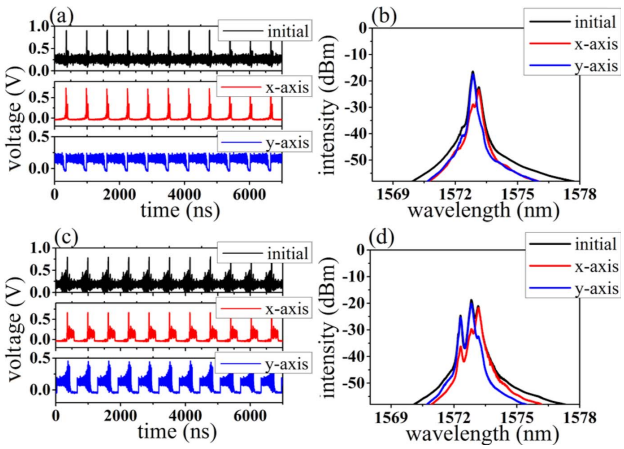


**Fig. 2.** (a), (c) The two orthogonal polarization states of the PDs with different durations and (b), (d) the corresponding spectra.

resulted from the group velocity matching so that the two components on the fast and slow axes of the fiber can propagate together without breakup. Adjusting the intracavity PC would affect the spectral filtering effect and change the laser operation state. When we rotated the PC1 slightly, the PD durations and the corresponding spectral distributions of the two orthogonal components would change, as shown in Figs. 2(c) and 2(d). The temporal profiles of the PDs evolved into rectangle-like pulses with side spikes, and the domain durations were 195 and 360 ns, respectively. The central wavelengths of the two orthogonal components were 1572.83 and 1573.17 nm, respectively, and the wavelength difference was 0.34 nm, which had a small offset compared with the previous state, as shown in the Fig. 2(b).

As the pump power was increased to 150 mW, the cross-polarization coupling strength increased, the PDs split, and the second-harmonic PDs were obtained. As shown in Fig. 3(a), the PDW pulse split to form a subdomain that was weaker than the main pulse. Figure 3(b) shows the corresponding spectra with the central wavelengths at 1573.22 and 1572.77 nm. The central wavelength difference was 0.45 nm, which also showed that the PDs resulted from incoherent mode coupling.

In order to study the evolution of the PDs with the birefringence varying, we fine-tuned the PC1 to adjust the birefringence in the cavity and kept the pump power unchanged. When we continuously adjusted the PC1, there were six representative

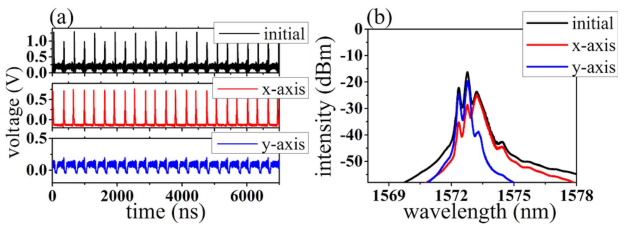


**Fig. 3.** (a) The temporal traces of the two orthogonal polarization modes and (b) the corresponding spectra.

states, as shown in Fig. 4. Especially, we found that a self-mode-locked pulse evolved from the PDs. Figure 4(a) is a typical PDW pulse, and the two orthogonal polarization components are rectangle-like pulses with noise-like spikes. Figure 4(b) shows the spectra of the pulse and the two polarization components; the wavelength difference between the two components was ~1.09 nm. When the PC1 was continuously rotated about 1.8° in one direction, the duration of the PD $x$ axis component

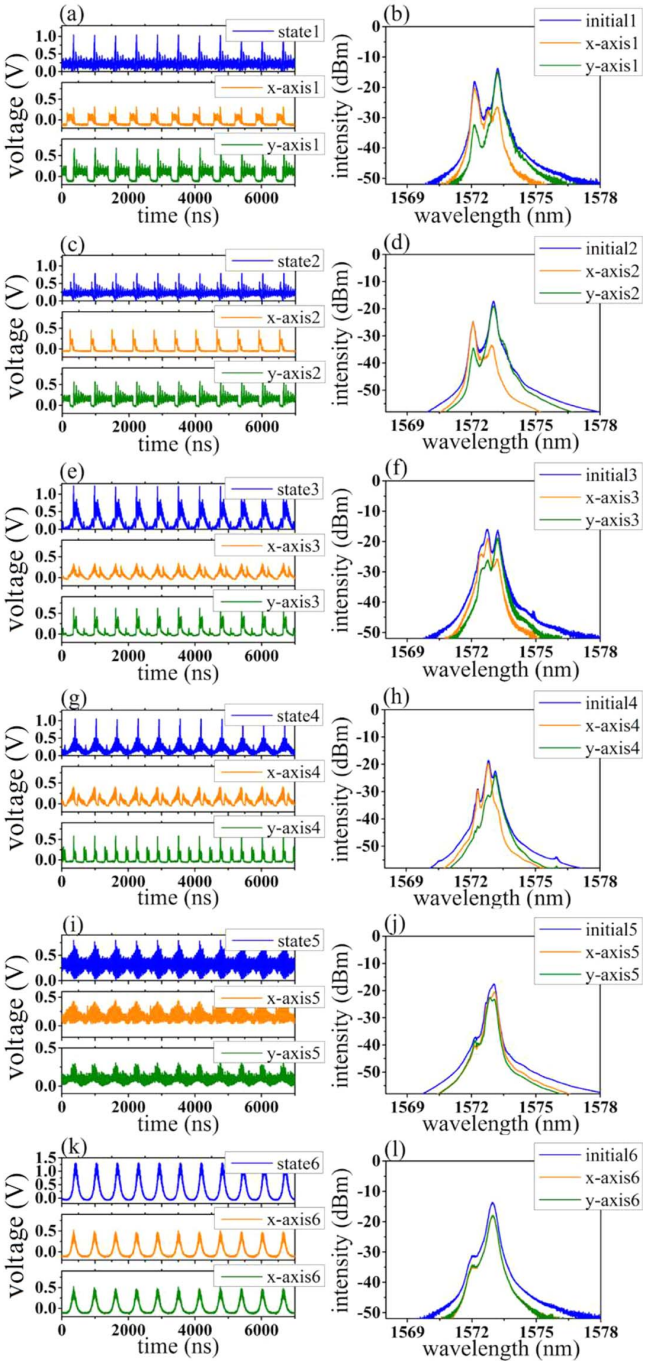


**Fig. 4.** (a), (c), (e), (g), (i), (k) The temporal traces of the two orthogonal polarization states and (b), (d), (f), (h), (j), (l) the corresponding spectra for different orientations of PC1.

decreased. In the meantime, the duration in the $y$ axis direction increased, as shown in Fig. 4(c). Figure 4(d) shows the corresponding spectra. Similarly, the two orthogonal polarization components had different spectral distributions, and the wavelength difference was 0.96 nm. Compared to the case in Fig. 4(b), the wavelength difference decreased, indicating that the intracavity birefringence decreased. From Figs. 4(e) and 4(g), corresponding to the PC rotation angles of 5.9° and 10.1°, we can find that the noise pulse evolved into a subdomain, which appeared on the right sides of the two orthogonal PDs. The domain wall, which was obtained by the superposition of the two orthogonal polarization components, formed a bright pulse with a strong substrate. Their spectra are shown in Figs. 4(f) and 4(h), where one can find the central wavelength differences of the two components were 0.48 and 0.32 nm, respectively. Further adjusting the PC1, we achieved a pulse bunch, shown in Fig. 4(i) at the rotation angle of 12.5°. The internal structure of the pulses exhibited a chaotic distribution of multidomain pulses. The corresponding spectra are shown in Fig. 4(j). The two orthogonal components had a wavelength difference of 0.21 nm. When the PC was finally rotated about 20.9°, the complex pulse structure disappeared, and the wavelength separation turned to zero, as shown in Figs. 4(k) and 4(l). The two orthogonal polarization components were both giant bright pulses with overlapped spectra centered at 1572.94 nm. During the whole adjustment process, the wavelength difference of the orthogonal components decreased, as shown in Fig. 5. The smaller the cavity birefringence, the smaller the wavelength difference between the two polarization components. Once the net birefringence difference was close to zero, the PD disappeared to form a stable giant mode-locked pulse.

It can be seen from Fig. 4(k) that the self-pulse period was about 633 ns and the repetition frequency was at 1.58 MHz, which were, respectively, equal to the laser round-trip time and the 1.58 MHz longitudinal mode interval determined by the 130 m cavity length, indicating that the laser operated at a self-mode-locked state. Keeping the state of PC1 unchanged and increasing the pump power, the pulse trains remained stable and the pulse repetition frequency also kept the same, which was consistent with the characteristics of mode-locked states. The spectra at different pump powers are shown in Fig. 6(a). The central wavelength was 1572.94 nm. As the pump power was gradually increased, both the output power and spectral width gradually increased, as shown in Fig. 6(b). We can observe that the maximum output power is up to 20 mW, and the maximum pulse energy is calculated to be ~12.66 nJ, which is higher than the energy of the general mode-locked pulse reported previously[34–36]. With the increase of the pump power, the nonlinear effects such as the self-phase modulation in the fiber cavity became stronger, which made the laser spectrum gradually broaden. The radio-frequency (RF) spectrum is shown in Fig. 6(c). The signal-to-noise ratio (SNR) was ~56 dB at the frequency of 1.58 MHz, which indicated that the pulse train was fairly stable. We also found that there were no periodic changes in the intensity of the two orthogonal components and no polarization evolution frequency components in the RF spectrum, as shown in the Fig. 6(c). So the self-mode-locked pulse was the polarization-locked vector pulse[37]. Since the self-mode-locked pulse width was obviously wide, which was beyond the measurement range of the autocorrelator, we measured the pulse duration roughly using a 28 GHz high-speed oscilloscope. The measured pulse shape and its Gaussian fitting curve are shown in Fig. 6(d), where it can be seen that the full width at half-maximum of the pulse was about 143 ns.

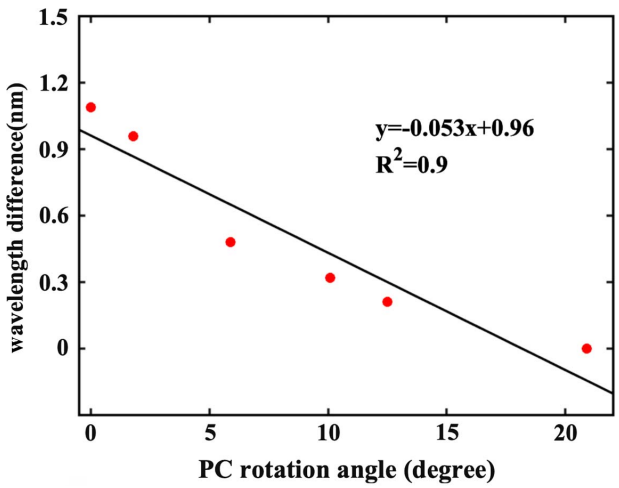


Fig. 5. Wavelength differences under different PC states.

## 4. Discussion

Since there was no polarization-dependent loss device in our fiber laser cavity, the two orthogonal polarization components in the cavity always oscillated simultaneously under steady laser operation state. PDs were formed due to the incoherent

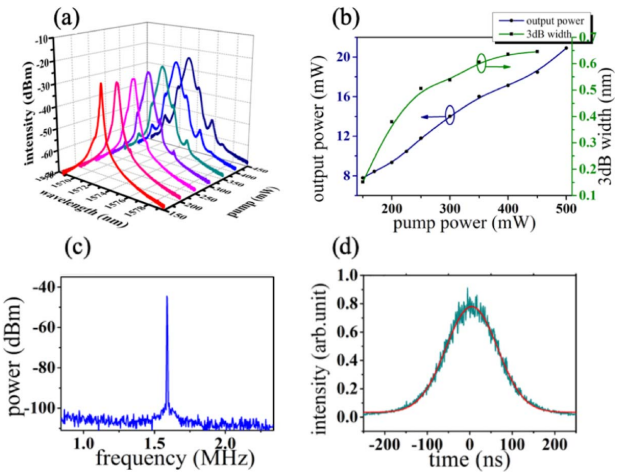


Fig. 6. (a) Spectra of the self-mode-locked pulse under different pump powers; (b) 3 dB width and laser output power versus the pump power; (c) corresponding RF spectrum; (d) pulse shape detected by a 28 GHz high-speed oscilloscope (the red curve is the Gaussian fitting).

cross-polarization coupling between the two orthogonal polarization modes[7–9]. The duration of PDs can be controlled through regulating the birefringence by rotating the PC1.

From the experimental results shown in Fig. 4, by adjusting the PC1, the PDs passed through states of rectangle-shaped PDs, PDs with noise-like spikes, PDs with subdomain pulses, and pulse bunches with complex multidomain pulse structures. As the birefringence gradually decreased by fine-tuning the PC1, the wavelength difference between the two polarization components decreased and the cross-polarization coupling strength increased. With the increase of the coupling strength, the PDs gradually split into subdomain pulses and eventually broke up into chaotic multidomains. When the cavity birefringence was close to zero, the PD structure disappeared to form a giant bright pulse with a fundamental repetition frequency. The giant bright pulse with nanosecond duration was not a single soliton, whose width was usually in the range of picoseconds or narrower. Due to the limitation of the device bandwidth, the fine structure inside the pulse cannot be displayed. According to the evolution process, shown in the Figs. 4(i)–4(l), we speculated that the self-mode-locked pulse originated from the multidomain structures that were split from the PDs.

The whole evolution process from the PDs to the giant self-mode-locked pulse is as follows. Under relatively weak coupling, there were only two PDs; each domain pulse corresponds to one of the orthogonal polarizations. When continuously adjusting the PC1 to gradually reduce the cavity birefringence, the wavelength difference between the two polarization components decreased, resulting in stronger cross coupling between polarization modes. Under strong coupling, the PD splitting occurred and subdomain pulses were obtained[22]. When the coupling strength was strong enough, the PDs broke up and split into irregular multidomains with complex distribution structures. The polarization switching points were blurred due to the chaotic distribution of the subdomains. When the birefringence was close to zero, the group velocity matching condition was relaxed, and the spectra of two polarization components were almost coincident[10]. The incoherent cross coupling between polarization modes transformed into coherent coupling with stronger coupling strength[9]. In addition, the hundred-meter long fiber used in the cavity also enhanced the nonlinear optical effect[38,39] and further strengthened the cross-polarization coupling. Under this condition, the fixed phase relationship between neighboring longitudinal modes formed due to the strong mode coupling and then the self-mode-locked pulse was achieved.

## 5. Conclusions

In conclusion, we have investigated various vector pulses observed in a 130 m long erbium-doped fiber laser without any polarization-dependent loss elements. We have achieved various PDs with different domain durations and spectral distributions by adjusting the intracavity PC1. By fine-tuning the intracavity PC1, we studied the detailed evolution process of the PDs with the cavity birefringence varying. As the birefringence gradually decreased, the PDs split into multidomain pulses and eventually evolved into a giant self-mode-locked pulse. The self-mode-locked pulse was at a fundamental repetition frequency of 1.58 MHz and possessed a high pulse energy of 12.66 nJ. The SNR was 56 dB, which indicated that the self-mode-locked pulse had good stability. For the first time, we found that the self-mode-locked pulse can evolve from the PDs by adjusting the intracavity PC. We speculated that this self-mode-locked pulse originated from the multiple subdomain pulses. Due to the strong coherent coupling between two polarization modes, the PDs were split to obtain multidomains with chaotic distributions and formed a fixed phase relationship, which manifested as a single giant bright pulse oscillating at the fundamental frequency. Our work deepens our understanding of the PD phenomena in fiber lasers and provides a new perspective to explain the formation of the self-mode-locked pulse.

## Acknowledgement

This work was supported by the National Key Research and Development Program of China (No. 2018YFE0117400), National Natural Science Foundation of China (No. 62275093), and China Postdoctoral Science Foundation (No. 2018M642823).

## References

1. R. I. Woodward and E. J. R. Kelleher, "2D saturable absorbers for fibre lasers," Appl. Sci. **5**, 1440 (2015).
2. A. Martinez and Z. Sun, "Nanotube and graphene saturable absorbers for fibre lasers," Nat. Photon. **7**, 842 (2013).
3. M. E. Fermann, F. Haberl, M. Hofer, and H. Hochreiter, "Nonlinear amplifying loop mirror," Opt. Lett. **15**, 752 (1990).
4. Y. Du, X. Shu, and Z. Xu, "All-fiber passively mode-locked laser based on a chiral fiber grating," Opt. Lett. **41**, 360 (2016).
5. X. Feng, H. Tam, and P. K. A. Wai, "Stable and uniform multiwavelength erbium-doped fiber laser using nonlinear polarization rotation," Opt. Express **14**, 8205 (2006).
6. H. Zhang, D. Y. Tang, L. M. Zhao, and X. Wu, "Observation of polarization domain wall solitons in weakly birefringent cavity fiber lasers," Phys. Rev. B **80**, 052302 (2009).
7. H. Zhang, D. Y. Tang, L. M. Zhao, and R. J. Knize, "Vector dark domain wall solitons in a fiber ring laser," Opt. Express **18**, 4428 (2010).
8. H. Zhang, D. Y. Tang, L. M. Zhao, and X. Wu, "Dual-wavelength domain wall solitons in a fiber ring laser," Opt. Express **19**, 3525 (2011).
9. D. Y. Tang, Y. F. Song, J. Guo, Y. J. Xiang, and D. Y. Shen, "Polarization domain formation and domain dynamics in a quasi-isotropic cavity fiber laser," IEEE J. Sel. Top. Quantum Electron. **20**, 42 (2014).
10. C. Lecaplain, P. Grelu, and S. Wabnitz, "Polarization-domain wall complexes in fiber lasers," J. Opt. Soc. Am. B **30**, 211 (2013).
11. C. Lecaplain, P. Grelu, and S. Wabnitz, "Dynamics of the transition from polarization disorder to antiphase polarization domains in vector fiber lasers," Phys. Rev. A **89**, 063812 (2014).
12. Z. B. Lin, A. P. Luo, S. K. Wang, H. Y. Wang, W. J. Cao, Z. C. Luo, and W. C. Xu, "Generation of dual-wavelength domain-wall rectangular-shape pulses in HNLF-based fiber ring laser," Opt. Laser Technol. **44**, 2260 (2012).
13. H. H. Liu and K. K. Chow, "Dark pulse generation in fiber lasers incorporating carbon nanotubes," Opt. Express **22**, 29708 (2014).
14. P. Wang, K. J. Zhao, X. S. Xiao, and C. X. Yang, "Pulse dynamics of dual-wavelength dissipative soliton resonances and domain wall solitons in a Tm fiber laser with fiber-based Lyot filter," Opt. Express **25**, 30708 (2017).

15. J. M. Liu, X. L. Li, S. M. Zhang, H. Zhang, P. G. Yan, M. M. Han, Z. G. Pang, and Z. J. Yang, "Polarization domain wall pulses in a microfiber-based topological insulator fiber laser," Sci. Rep. **6**, 29128 (2016).
16. M. Han, X. Li, and S. Zhang, "Polarization domains and polarization locked vector solitons in a fiber laser," IEEE Photon. Technol. Lett. **29**, 2230 (2017).
17. X. R. Zhu, B. Zhang, D. S. Zhao, L. Y. Yang, S. L. Liu, and J. Hou, "Pulse evolution and multi-pulse state of coherently coupled polarization domain walls in a fiber ring laser," Opt. Express **29**, 30558 (2021).
18. W. Y. Zhang, L. Zhan, T. H. Xian, and L. R. Gao, "Harmonic mode-locking in bidirectional domain-wall soliton fiber lasers," J. Light. Technol. **37**, 5417 (2019).
19. X. Li, S. Zhang, H. Han, M. Han, H. Zhang, L. Zhao, F. Wen, and Z. Yang, "Different polarization dynamic states in a vector Yb-doped fiber laser," Opt. Express **23**, 10747 (2015).
20. G. D. Shao, Y. F. Song, L. M. Zhao, D. Y. Shen, and D. Y. Tang, "Soliton-dark pulse pair formation in birefringent cavity fiber lasers through cross phase coupling," Opt. Express **23**, 26252 (2015).
21. X. Hu, J. Ma, L. M. Zhao, J. Guo, and D. Y. Tang, "Collision between soliton and polarization domain walls in fiber lasers," Opt. Express **29**, 12590 (2021).
22. X. Hu, J. Guo, J. Ma, L. Li, and D. Y. Tang, "Polarization domain splitting and incoherently coupled dark-bright vector soliton formation in single mode fiber lasers," J. Opt. Soc. Am. B **38**, 24 (2021).
23. M. Gilles, P. Y. Bony, J. Garnier, A. Picozzi, M. Guasoni, and J. Fatome, "Polarization domain walls in optical fibres as topological bits for data transmission," Nat. Photon. **11**, 102 (2017).
24. H. J. Baker and T. A. King, "Mode-beating in gain-switched iodine photodissociation laser pulse," J. Phys. D **8**, L31 (1975).
25. P. Myslinski, J. Chrostowski, J. A. K. Koningstein, and J. R. Simpson, "Self-mode locking in a *Q*-switched erbium-doped fiber laser," Appl. Opt. **32**, 286 (1993).
26. S. Collin, E. Contesse, P. L. Boudec, G. Stephan, and F. Sanchez, "Evidence of a saturable-absorption effect in heavily erbium-doped fibers," Opt. Lett. **21**, 1987 (1996).
27. R. Rangel-Rojo and M. Mohebi, "Study of the onset of self-pulsing behavior in an Er-doped fiber laser," Opt. Commun. **137**, 98 (1997).
28. M. Duran-Sanchez, B. Posada-Ramirez, RI. Alvarez-Tamayo, H. Santiago-Hernandez, M. Bello-Jimenez, B. Ibarra-Escamilla, S. Das, A. Dhar, M. Pal, M. C. Paul, A. V. Kir'yanov, and E. A. Kuzin, "Soliton molecules in self-mode-locked ring-cavity Er/Yb double-clad fiber laser," IEEE Photon. J. **11**, 1504608 (2019).
29. X. Zhang, S. L. Shu, K. D. Cai, Y. J. Wang, and C. Z. Tong, "Pulse control in self-mode-locked 2.8 mm Er-doped fluoride fiber lasers," Opt. Laser Technol. **129**, 106285 (2020).
30. C. Liu, Z. Q. Luo, Y. Z. Huang, B. Qu, H. H. Cheng, Y. Wang, D. D. Wu, H. Y. Xu, and Z. P. Cai, "Self-mode-locked 2 mm $Tm^{3+}$-doped double-clad fiber laser with a simple linear cavity," Appl. Opt. **53**, 892 (2014).
31. H. R. Zhang, J. J. Zhang, S. Z. Sun, D. D. Wu, R. W. Zhao, R. P. Wang, and S. X. Dai, "Self-mode-locking and self-phase modulation in $Tm^{3+}$-doped double clad fiber laser for pulse peak power enhancement and multi-wavelength generation," Opt. Laser Technol. **141**, 107128 (2021).
32. Y. Tang and J. Xu, "Effects of excited-state absorption on self-pulsing in $Tm^{3+}$-doped fiber lasers," J. Opt. Soc. Am. B **27**, 179 (2010).
33. D. C. Kirsch, A. Bednyakova, P. Varak, P. Honzatko, B. Cadier, T. Robin, A. Fotiadi, P. Peterka, and M. Chernysheva, "Gain-controlled broadband tuneability in self-mode-locked Thulium-doped fibre laser," Commun. Phys. **5**, 219 (2022).
34. H. Zhang, D. Y. Tang, L. M. Zhao, Q. L. Bao, and K. P. Loh, "Large energy mode locking of an erbium-doped fiber laser with atomic layer graphene," Opt. Express **17**, 17630 (2009).
35. K. Jiang, C. Ouyang, P. P. Shum, K. Wu, and J. H. Wong, "High-energy dissipative soliton with MHz repetition rate from an all-fiber passively mode-locked laser," Opt. Commun. **285**, 2422 (2012).
36. J. K. Chen, Z. K. Wang, L. J. Li, D. N. Wang, T. Y. Zhu, F. Gao, S. Y. Cao, and Z. J. Fang, "GIMF-based SA for generation of high pulse energy ultrafast solitons in a mode-locked linear-cavity fiber laser," J. Light. Technol. **38**, 1480 (2020).
37. S. T. Cundiff, B. C. Collings, and W. H. Knox, "Polarization locking in an isotropic mode locked soliton Er/Yb fiber laser," Opt. Express **1**, 12 (1997).
38. X. Li, X. Liu, X. Hu, L. Wang, H. Lu, Y. Wang, and W. Zhao, "Long-cavity passively mode-locked fiber ring laser with high-energy rectangular-shape pulses in anomalous dispersion regime," Opt. Lett. **35**, 3249 (2010).
39. S. Kobtsev and S. Smirnov, "Fiber lasers mode-locked due to nonlinear polarization evolution: golden mean of cavity length," Laser Phys. **21**, 272 (2011).